Feasibility of ultrasonic non-destructive testing of ancient funerary urns : experimental and analytical parametric model

Philippe Lasaygues, Elise Doveri, Matthieu Boutoille, Jacques Rebière, Cécile Baron, Paul Bailet

Feasibility of ultrasonic non-destructive testing of ancient funerary urns : experimental and analytical parametric model

Philippe Lasaygues[a,*], Elise Doveri[a], Matthieu Boutoille[a], Jacques Rebière[b], Cécile Baron[c], Paul Bailet[d]

[a]*Aix Marseille Univ, CNRS, Centrale Marseille, LMA UMR 7031, 4 impasse Nikola Tesla, 13453, Marseille, France*
[b]*Laboratoire de conservation, restauration et recherches, 19 Rue Frédéric Mireur, 83300, Draguignan, France*
[c]*Aix Marseille Univ, CNRS, Centrale Marseille, IRPHE UMR 7342, 49 rue Frédéric Joliot-Curie, 13384, Marseille, France*
[d]*Dracénie Provence Verdon agglomération, Université Nice Sophia Antipolis, CNRS-UNS, CEPAM UMR 7264, 24, avenue des Diables Bleus, 06300, Nice, France*

Abstract

Non-invasive modalities are being developed as the computer tools and industrial non-destructive testing capabilities become more widespread. Using the same investigation methods as those applied to modern objects, we seek to study ancient funerary urns containing human bones. The exploration of ancient urns is key to increasing our understanding of the practices of burial and cremation in archaeo-anthropology. But those urns present at archaeological sites are exposed to diversified environments (wet, temperate or dry environment), and can be subjected to chemical or mechanical destructive actions over time. As ancient funeral urns containers are sometimes made of lead, stone or ceramic, the use of X-ray scanners is difficult or even impossible for *in situ* control. In this work, we propose an engineering technique based on ultrasonic non-destructive testing and wave propagation in urns. An analytical parametric model is developed using mathematical signal processing tools and validated by means of laboratory experiments under controlled conditions of propagation through artificial urns for two ultrasonic frequencies (500 kHz and 1 MHz). The aim is to characterise an ancient urn by creating an analytical model, and to use a parametric identification algorithm to determine the presence or absence of bone fragments. The parametric identification algorithm based on the Levenberg-Marquardt method makes it possible to determine the geometrical (thickness) and physical (wave velocity and

*Corresponding author

Email addresses: lasaygues@lma.cnrs-mrs.fr (Philippe Lasaygues), doveri@lma.cnrs-mrs.fr (Elise Doveri), matthieuboutoille@outlook.fr (Matthieu Boutoille), lc2r.conservation@orange.fr (Jacques Rebière), cecile.baron@univ-amu.fr (Cécile Baron), paul.bailet@dracenie.com (Paul Bailet)

attenuation, mass density) parameters when the urn is filled with water, with water and bones, and with water, bones and sand. We show that the model makes it readily (processing time ≈ 15 sec) possible to find the different times of flight between the transducer and the different walls of the urn and the parameters with an accuracy less than 10%.

Keywords: Non-destructive testing, Ultrasonic waves, Parametric model, Ancient funerary urn

1. Introduction

The exploration of ancient funerary urns is key to increasing our understanding of the practices of inhumation and cremation in archaeo-anthropology, and to understanding past human societies, [1], [2], [3] and [4]. For a long time, tomb excavation only aimed to reveal ancient funerary objects. But after years of archaeological research, the study of bone fragments has become the most important element of funerary archaeo-anthropology. The characterisation of ancient funerary urns and fragments provides information not only about the lives of individuals, but also about the evolution of an entire society. Anthropological excavation greatly expanded in the 1980s, focusing on bone fragments and skeletons, and more particularly on skeletal (sarcophagi, for example) and bone (funerary urns) receptacles. While the main aim of funerary archaeology is to reconstruct funerary gestures, field anthropology focuses on bone remains and aims to reconstruct skeletons and their relationship with funerary artefacts. Based on the contents and natures of the bones, it attempts to reconstruct the various funerary rites and the different layouts of a grave or burial site. But tombs, and/or the artefacts found at archaeological sites such as urns, may be exposed to humid, temperate or dry environments, and possibly to destructive chemical or mechanical action over time.

Depending on these archaeological facts, the issues developed and the time available, excavation and laboratory investigation procedures have to evolve and adapt. Archaeoscience borrows principles and methods from life and earth sciences, from biological and chemical sciences, and from medical and medico-legal sciences, [5]. Archaeoscience takes into account a large number of macroscopic, microscopic and molecular indicators, both organic (plants, animals, humans) and inorganic (minerals, metals). Most often, because of their complex protocols, these methods have to be carried out in the laboratory using specific instruments, which can be heavy and expensive, such as medical scanners. There are very few *in situ* methods other than photography, photogrammetry and the simple but highly effective method of drawing.

Non-invasive methods are being developed as computer and digital tools, and non-destructive testing (NDT) capabilities become more advanced and widespread. In the same way as industrial NDT has been used on manufactured objects, X-ray tomodensitometry is being used in the laboratory on ancient funerary urns containing human bones, [6], [7], [8], and [9]. Because ancient funerary urns are sometimes bowls made of lead, stone, or ceramic, the use of X-ray modalities to determine the presence or absence of bone fragments of anatomical elements is difficult, and nearly impossible for *in situ* exploitation. Anthropologists who

practice and manage sections of human archaeology are therefore interested in alternative, non-destructive approaches that would allow them to analyse remains and specimens in the laboratory and/or *in situ* without damage or destruction.

Ultrasound techniques are particularly adapted for bone characterisation. There is a substantial literature on the characterisation of bones by propagative methods, [10], but in this case the bones are often fresh or the post-mortem delays are short ($<$ 1 year on average). There is no suitable method for the study of older, antique or even prehistoric bone fragments, even less so when they have been conditioned or transformed.

In this work, ultrasonic wave propagation in funerary urns was studied. First, an analytical model was developed using mathematical tools for signal processing, and validated by means of laboratory experiments under controlled conditions of propagation through artificial urns. Second, an optimisation algorithm of the difference between model and measures, enabled us to evaluate the geometrical (thickness) and physical (mass density, ultrasonic wave velocity and attenuation) parameters of the urn, and to detect the presence or absence of bones inside it.

The optimisation algorithm, based on the Levenberg-Marquardt procedure for minimising the difference between the ultrasonic wave recorded at a position around the urn, and the corresponding numerical modelled signal, enabled us to calculate the 4 unknown geometrical and physical parameters of the urn, and to detect the presence of bones inside it. This parametric identification algorithm converged rapidly in less than fifteen seconds, which made it possible to identify an urn and its contents with an acceptable degree of accuracy (deviation lower than 20$\%$) for *in situ* exploitation. Three artificial clay urns, one empty, one containing bones, and one containing bones and sand, were used in this study. The study comprised 4 steps:

- proposition of a representative **analytical model** of the interaction of an ultrasonic wave with an urn.
- development of an **optimisation algorithm** for **parametric identification** of the urn.
- study of the **convergence** of the method for 3 configurations (empty urn, urn containing bones, and urn containing bones and sand).
- study of the **relevance, reproducibility** and the **resistance** of the model and the identification algorithm for several measurement points around the urn.

2. Materials &Methods

2.1. Description of the urns

Three artificial urns reproducing ancient funerary ceramics were used, made of (*terracotta*) clay by a potter specialized in archaeology, (Figures 1 and 2). The urns were built in successive homogeneous clay layers, whose thicknesses and heights differed by a few millimeters. The dimensions of the urns, measured with a caliper at several points, were approximately identical. The outer diameter, D_{out}, was 130$\pm$0.2 mm. The height of the urns was 135$\pm$0.03 mm. The thickness, E_{urn}, of the urn walls was measured for each urn separately using a caliper. The first urn was empty, the second contained only bones and the third contained bones and coarse sand (average particle size more than 0.5 mm). The bones were fragments of real human bones from Hammamet in Tunisia (1st century AD), composed of different pieces, such as femoral heads, lower jaws, diaphysis of tibias or fibulae, flat bones such as scapulae, and vertebrae.

Figure 1: Photos of the artificial funerary urns, empty (left), containing bones (centre), containing bones and sand (right).

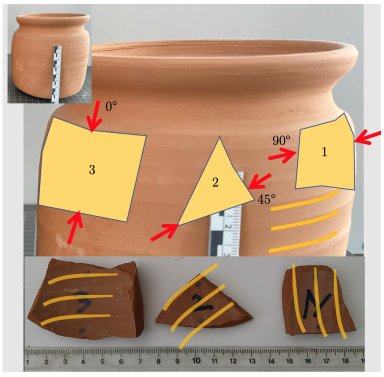

Figure 2: Orientation of the clay layers in an artificial funerary urn manufactured according to the concepts of the 1st century AD. The yellow lines represent the orientation of the layers in the clay samples. The red arrows represent the chosen orientation of the axis, so that it is perpendicular to the acoustical beam when measuring the acoustical parameters of the clay.

2.2. Ultrasonic non-destructive testing devices

2.2.1. 1MHz configuration: Ultrasonic electro-mechanical 2D-scanner

Ultrasonic experiments were performed in echo mode using an ultrasonic electro-mechanical 2D-scanner with a horizontal main arm carrying a vertical support holder for a 1MHz-transducer, (Figure 3). The transducer and holder were immersed in a circular water tank of 2m diameter. The temperature of the water ranged from 21°5 to 21°7, and the reference velocity, V_{water}, of the ultrasonic wave in water was 1474$\pm$1 m/s.

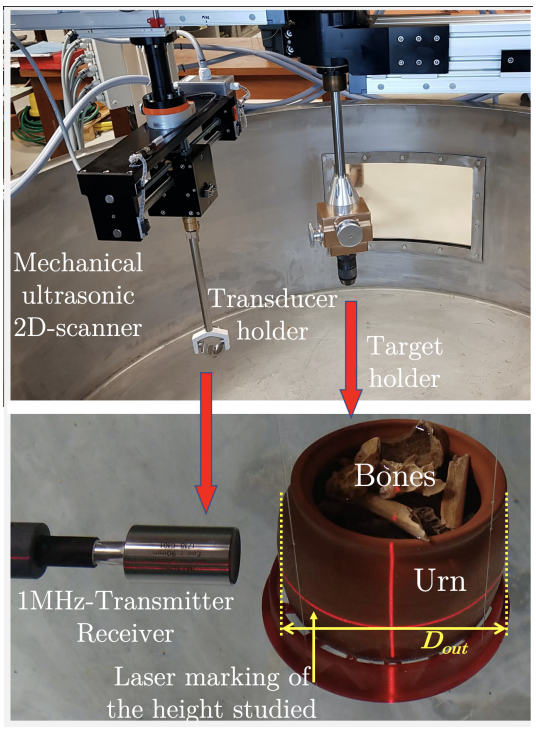

Figure 3: Photos of the ultrasonic electro-mechanical 2D-scanner and the bone-containing urn placed at the centre.

By means of stepping motors and an electronic motorization rack (Rhonax, Thyez, France) to manage the mechanical displacements, the transducer could be adjusted and moved linearly relative to the tested urn positioned at the geometrical centre of the scanner. The urns, whether they were empty or containing bones and no sand or bones and sand, were immersed in the water tank, so that their inner cavity was always filled with water, whatever else they contained.

2.2.2. 500kHz configuration: Portable inspection unit

A second ultrasonic experiment was carried out, again in echo mode, using a portable inspection unit (diameter of 170 mm, height of 150 mm) consisting of a 3D-printed support to position a 500kHz-transducer in contact with the urn. To ensure the wave transmission with the minimum loss of energy, a 2cm-thick gel pad (Aquaflex^{TM}, Parker laboratories INC, Fairfield, USA) used for medical applications, was placed between the front of the transducer and the urn.

Figure 4: Photos of the ultrasonic portable inspection unit and the funerary urn inside, when the inner cavity was filled with water (right), and water and bones (left).

2.2.3. Transducer and electro-acoustical devices

The transducers (Imasonic, Voray-sur-l'Ognon, France) were piezo-composite transducers with a nominal frequency, f_0, of 1 MHz, and 500 kHz. The -6 dB-bandwidths were of 1.5 MHz (from 0.5 MHz to 2 MHz), and 530 kHz (from 230 kHz to 760 kHz). The 1MHz-transducer had a housing height of 60 mm and a diameter of 40 mm (active diameter of 30 mm) (Figure 5-a), a focal length of 90 mm in the Fresnel zone, an aperture (axial (0x) and lateral (0y)) of 4.6 mm and a slice thickness (0z) of 3 mm. The 500kHz-transducer was 55 mm high and 45 mm in diameter (active diameter 42 mm) (Figure 5-b). The shape and dimensions of the acoustical field of this contact transducer are not relevant. Each transducer was used as a transmitter to send a incident wave, then as a receiver to record the waves reflected by the urn.

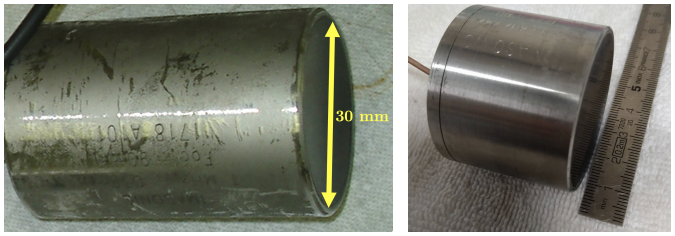

(a) **(b)**

Figure 5: Photos of the 1 MHz (left) and 500 kHz (right) ultrasonic transducers.

Each transducer was driven using a pulse-receiver generator (Sofranel 5077 PR, Olympus, USA) including the voltage amplifier. The radio-frequency signals (RF-signals) were conveyed from the 12-bit oscilloscope (Lecroy HDO 6104, Teledyne Inc., Thousand Oaks, CA, USA), including the data digitizer, to a personal computer using a USB interface file transfer, and stored. Each RF-signal contained N=4096 samples, and the sampling frequency, F_e, was 20 MHz. The voltage amplifier delivered an output voltage from 40 mV_{pp}. The envelope was defined by the modulus of the Hilbert transform of the RF-signal. All processing algorithms were implemented using Matlab® (The MathWorks, Inc., Natick, Massachusetts, USA).

2.3. Analytical ultrasonic 1D-model

2.3.1. General synoptic

Figure 6 shows the synoptic diagramme of the non-destructive echo-mode testing system of a funerary urn.
The electro-mechanical and electro-acoustical devices and the transducer therefore serve as a continuous, linear, stationary causal filter of the acoustical signature of the urn.

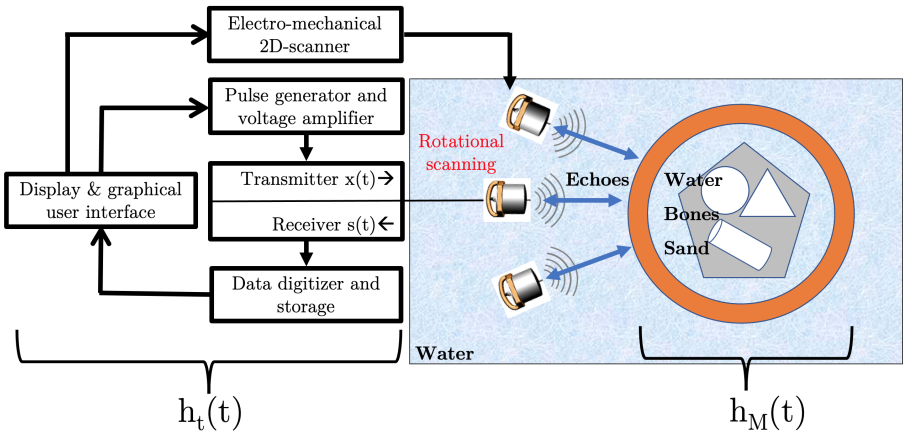

Figure 6: Synoptic diagramme of the non-destructive testing system.

The transmitted, x(t), and the recorded, s(t), signals are connected by convolution:

$$s(t) = x(t) \circledast h_M(t) \tag{1}$$

$$x(t) = h_t(t) \circledast e(t) \tag{2}$$

where $\circledast$ denotes the convolution operation.
h_M is the ultrasonic response of the urn studied. This variable is unknown, and its model and comparison with experimental measurements are the objectives of the proposed parametric ultrasonic non-destructive testing.
h_t is the electro-acoustical impulse response of the electro-acoustical acquisition system. It is assumed to be linear and known.
e, also known, is the electrical input conveyed to the transducer via the pulse generator. In pulse mode, this signal is comparable to a Dirac delta function, $\delta(t)$ (in terms of distribution), which is the neutral element of the convolution operation:

$$\delta(t) = \begin{cases} 1 & if\, t = 0 \\ 0 & if\, t \neq 0 \end{cases} \tag{3}$$

The transmitted signal, $x(t)$ (Eq. 2), can therefore be written as a copy of the electro-acoustical impulse response:

$$x(t) = h_t(t) \tag{4}$$

And the recorded signal, $s(t)$ (Eq. 1) can therefore be written as:

$$s(t) = h_t(t) \circledast h_M(t) \tag{5}$$

In this work, only the pure compression waves (which from now on will be called ultrasonic waves) were taken into account, and the shear waves propagating in the walls of the urn or in the bones fragments were considered negligible. The water, urns, bones and sand were considered to be weakly dispersive media/materials. As a result, attenuation was considered to be slightly different at 500 kHz and 1 MHz, while the wave velocities were taken to be constant and independent of the frequency. Only the propagation time (which from now on will be called the time of flight, TOF) and the amplitudes of the sound waves were modelled and measured.

2.3.2. Modelling of the electro-acoustical impulse responses of the devices

Lasaygues et al., [11], have shown that the electro-acoustical impulse response can be obtained by echo-mode measurements on objects that are infinite-dimensional (with respect to the wavelength) and perfectly reflecting, such as a large flat aluminum plate. In *in situ* NDT, the signal corresponding to the first back-and-forth travel between the transducer and the object under investigation is generally used as the electro-acoustical impulse response. This is a common means of calibrating ultrasonic NDT devices. But here, the object under investigation was an urn made of clay, and this material is not perfectly reflective. The first waves observed cannot be used to calibrate the device, and cannot be used as electro-acoustical impulse response.

In this work, the electro-acoustical impulse response of the devices was modelled using a pseudo-Ricker wavelet (damped sinusoid):

$$h_t(t) = sin(2\pi \frac{f_0}{F_e} t) exp(\frac{-t^2}{\sigma^2}) t \frac{1}{\sigma} \tag{6}$$

f_0 is the centre frequency of the transducer (1 MHz and 500 kHz, in this work), F_e is the sampling frequency (20 MHz in this work), and σ is a factor of the sampling frequency (F_e). Figures 7 and 8 show examples of a pseudo-Ricker wavelet with the parameters used in this work.

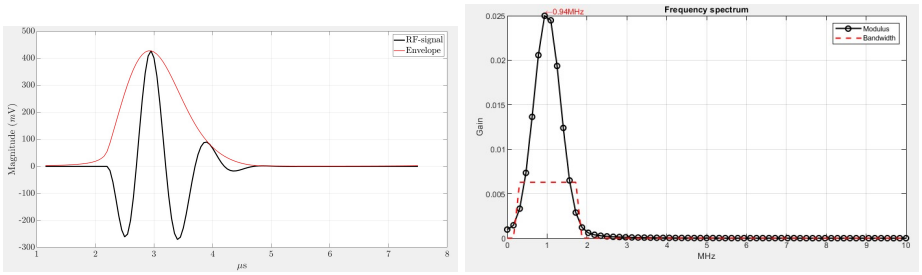

(a) **(b)**

Figure 7: Temporal and spectral representation of the pseudo-Ricker wavelet h_t (4096 samples, f_0=1 MHz, F_e=20 MHz, σ=20). The dotted red curve on the temporal representation represents the envelope of the signal (i.e., the modulus of the Hilbert transform). The dotted red line on the spectral representation marks the limits of the -6dB-bandwidth.

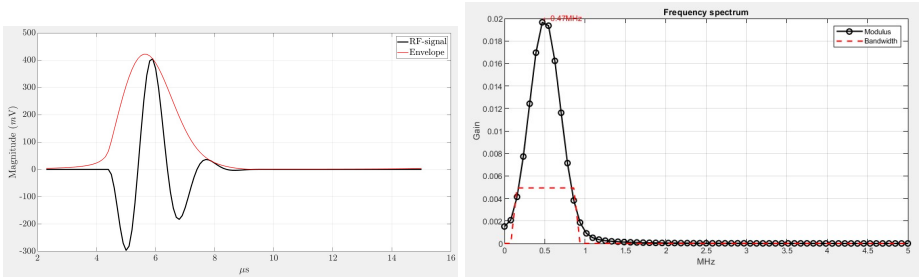

(a) **(b)**

Figure 8: Temporal and spectral representation of the pseudo-Ricker wavelet h_t (4096 samples, f_0=500 kHz, F_e=20 MHz, σ=20).The dotted red curve on the temporal representation represents the envelope of the signal (i.e., the modulus of the Hilbert transform). The dotted red line on the spectral representation marks the limits of the -6dB-bandwidth.

2.3.3. Modelling of the response of the urn

The funerary urns were placed in the centre of each device at a distance of $H = 86.5 \pm 0.4\, mm$ from the active surface of the 1MHz-transducer, in their Fresnel zone ($90\ mm$) (electro-mechanical 2D-scanner), or at the distance of 2 cm of the 500kHz-transducer front face (portable inspection unit). In this work, because of the narrow ultrasonic beam aperture, the effect of the side lobes was neglected. The waves reach the urn walls, which are assumed to be plane and perpendicular, with an almost plane wave front (i.e., the incidence angle was null). The walls of the urn were modelled by a succession of two infinite perfect rectangular parallelepipeds, perpendicular to the acoustical beams, of thickness, E_{urn}, equal to that

of the urn walls, and separated by a distance equal to that of their inner cavity, ($D_{\text{out}} - 2E_{\text{urn}}$). The parallelepipeds were supposed to be made of clay (Figure 9). The geometry of the bones contained in the urn was not known. The objective of the work was to determine the presence or absence of bones inside the urn, not their shape or the nature (whether burnt or not, for example) of the fragments. As a first approximation, the bones were therefore modelled by a medium whose properties were different from those of the empty urn containing water only. This inner medium was defined by its physical and acoustical parameters assumed to be known (ρ_{cavity}, V_{cavity} and α_{cavity}). These parameters would be prior parameters of the problem. The cavity was considered successively as being water, water and bones, and water, bones and sand.

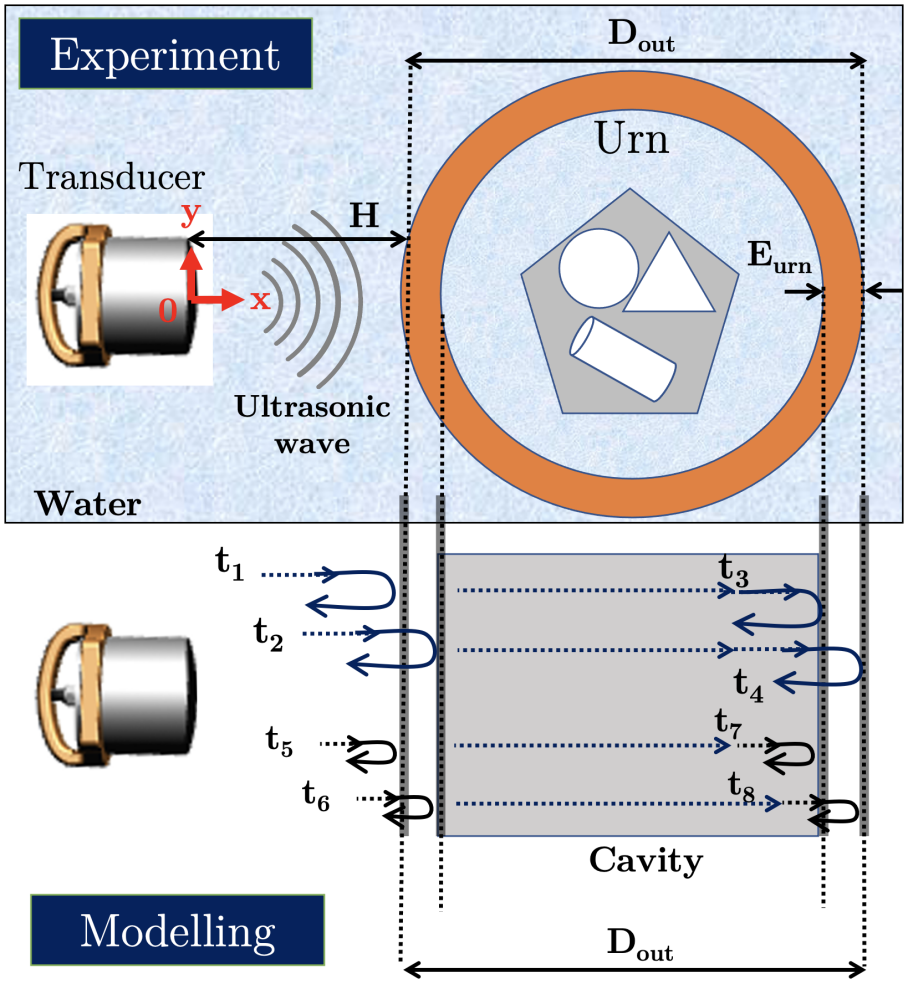

Figure 9: Schematic model of the ultrasonic non-destructive testing of a funerary urn using ultrasounds in echo mode.

The response $h_M(t)$ of the urn was modelled as the sum of pulse signals, which were comparable to Dirac delta functions (in terms of the distribution) :

$$h_M(t) = \sum_n A_n \delta(t - t_n) \tag{7}$$

where A_n were the amplitudes of the wave packets corresponding to the time-delays of the reflected waves, located at the TOF, t_n. The indices n were between 1 and 8. For indices n equal to 1 to 4, the values of the amplitudes, A_n, and

TOF, t_n, corresponded to the first four specular waves (direct waves) successively reflected on the four interfaces. In this work, the approximation for multiple reflected waves was limited to the order 2, which means that the back-and-forth travels corresponding to the reflection of waves on the interfaces beyond two times (multiple waves) were no longer recordable. Four multiple waves were then modelled for indices n equal to 5 to 8.

The TOF t_n depended on the velocity of the ultrasonic wave in the crossed medium (the water, V_{water}, the urn, V_{urn}, and the cavity V_{cavity}), the urn wall thickness, E_{urn}, the urn inner diameter, $D_{out} - 2E_{urn}$, and the distance between the transducer and the urn, H. For example, the TOF t_1 was corresponding to the time delay related to the first back-and-forth travel between the transducer and the first urn interface:

$$t_1 = 2\frac{H}{V_{water}} \tag{8}$$

The TOF t_2 was corresponding to the propagation through the water to the first urn interface in water, the propagation through the thickness of the urn at velocity V_{urn}, and the back travel to the transducer:

$$t_2 = 2(\frac{H}{V_{water}} + \frac{E_{urn}}{V_{urn}}) = t_1 + \frac{2E_{urn}}{V_{urn}} \tag{9}$$

Similarly, t_3 was computed as a function of t_2 by adding the propagation in the inner cavity inside the urn:

$$t_3 = t_2 + \frac{2D_{in}}{V_{cavity}} \tag{10}$$

The other TOF t_n, for $n = 4$ to 8, were calculated with the same formula, by adapting the number of back-and-forth travels.

The amplitudes A_n depended on the transmission and reflection coefficients on the considered interfaces (water/urn and cavity/urn), and on the wave attenuation coefficients in the media.
The coefficient of reflection of a wave on a medium 1/medium 2 interface was defined under normal incident conditions as:

$$R_{1,2} = \frac{[Z_2 - Z_1]^2}{[Z_2 + Z_1]^2} \tag{11}$$

and the transmission coefficient was defined as:

$$T_{1,2} = \frac{4Z_1Z_2}{[Z_2 + Z_1]^2} \tag{12}$$

where Z_1=$\rho_1 V_1$ and Z_2=$\rho_2 V_2$ were the acoustical impedances [$MRayls = kg/m^2/s$], of medium 1 and of medium 2. ρ was the mass density [kg/m^3], of the medium, and V was the velocity [m/s], of the ultrasonic wave propagating in the medium. Equation 12 was admitted by supposing that all the energies of the waves were reflected or transmitted, and that all the higher order phenomena of energy loss (heat, diffusion or dispersion) were neglected. The reflection and transmission coefficients were calculated at the water/urn and cavity/urn interfaces, at the water/transducer interface, and inside the wall thickness. These coefficients represent the energy distribution between the waves that cross the interface and those that are reflected. They are written as the ratio between the amplitudes of the reflected waves, A_n^R, (respectively transmitted waves, A_n^T), and the incident waves, A_n^I:

$$A_n^R = -A_n^I R \tag{13}$$

$$A_n^T = A_n^I T \tag{14}$$

The minus sign models the phase shift inversion of the acoustical signals during a reflection on an interface.
The amplitude $A_n(x_2)$ of a wave at the distance x_2 is a function of the initial amplitude $A_n(x_1)$ and the wave attenuation coefficient α [$dB/m/f_0$] of the wave over the distance $|x_2 - x_1|$:

$$A_n(x_2) = A_n(x_1)e^{-\alpha|x_2-x_1|} \tag{15}$$

The attenuation of the waves in the water and in the thickness of the urn wall was taken into account. The first amplitude, A_1, and the first TOF, t_1, corresponded to the first wave packet of the recorded signals, Indeed, the variables, H and V_{water} in Equation 8, were known, so that the first wave packet characterised precisely the first interface of the wall of the urn.

Identifying the variable h_M (Eq.7) consisted therefore in determining the geometrical parameter, E_{urn}, the physical parameter, ρ_{urn}, and the acoustical parameters, V_{urn} and α_{urn}. D_{out} was the known diameter of the urn, measured using a caliper. The physical parameters (ρ_{cavity}, V_{cavity} and α_{cavity}) of the inner cavity

containing either water, water and bones, or water, bones and sand were also a *prior* parameters.

2.4. Parametric identification algorithm

The parametric identification algorithm proposed in this work to identify the set of geometrical and physical parameters of the urn, was based on an adaptive iterative optimisation procedure. This procedure consisted in iteratively minimising a cost function, C, which was the difference between the signal recorded, s_{mea}, and the corresponding signal modelled, s_{mod} (Figure 10), and adapting the model at each iteration:

$$C = |s_{mea}(t) - s_{mod}(t)| \tag{16}$$

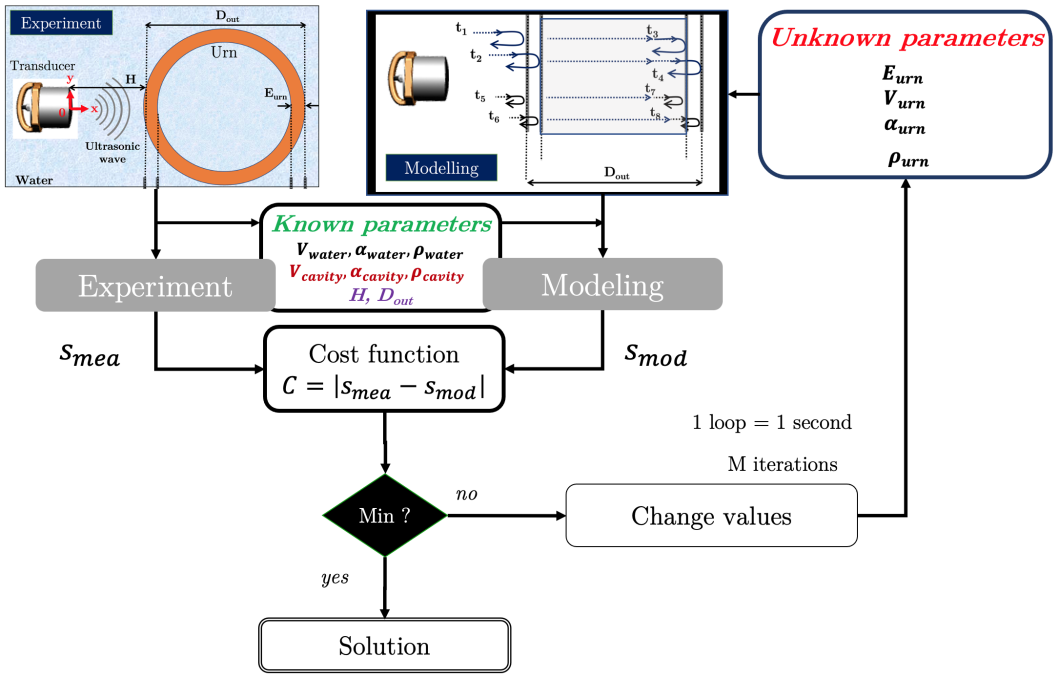

Figure 10: Adaptive iterative optimisation algorithm for the identification of the geometrical and physical parameters of a funerary urn.

The solution was calculated using an iterative algorithm for solving nonlinear least squares problems, based on the Levenberg-Marquardt method. The algorithm started with lower bound parameters given by the user, and found a minimum to the cost function, C. If this minimum was lower than the defined threshold

(10^{-5} in this study) then the algorithm stopped, and the parameters for that iteration were the estimated ones. Otherwise, the algorithm was continued iteratively by modifying the model parameters, until it reached the upper bound. If it reached the upper bound, there was no convergence and no solution found.

The parametric identification algorithm was studied in order to know the number of iterations needed, the speed of convergence to reach the threshold, and also the behaviour and the resilience of the solutions to transducer positioning variations. To test the convergence, the parameters obtained by the parametric identification algorithm had to be compared with experimental mean parameters for the urns and clay. These initial values were also used to define the lower and upper bounds of the algorithm. To study the behaviour of the algorithm as a function of the position on the urn, parametric identifications were carried out all around the urns at several positions in the same orthogonal plane.

2.5. Initial geometrical and physical parameters

In the study, two categories of geometrical and physical parameters were retained.

- The ***known*** or ***prior*** parameters were the distance, H, between transducer and urn, the ultrasonic wave velocity, V_{water}, and attenuation, α_{water}, in water, the mass density, ρ_{water}, of the water, the outer diameter of each urn, D_{out}, and the parameters of the inner cavity, V_{cavity}, α_{cavity}, and ρ_{cavity}, which could be water, bones, or bones and sand.

- The ***unknown*** parameters to be found were the thickness of each urn, E_{urn}, the ultrasonic wave velocity, V_{urn}, and attenuation, α_{urn}, in the clay parts, and the mass density, ρ_{urn}, of the clay.

The parameters to be found had previously been measured by independent methods on three clay pieces (figure 2) from an urn constructed identically to those studied, and the values were first compared with the literature, [12]. For each parameter, 10 measurements had been performed, and the mean values were used for the study.

- D_{out} and E_{urn} were measured with a caliper (Absolute Digimatik Solar®, Mitutoyo, Kanagawa, Japan).

- The ultrasonic wave velocities, V_{urn}, and attenuations, α_{urn} were measured by ultrasonic interferometry for both 500kHz- and 1MHz-frequency, based on the work of Lasaygues et al, [13].

- The mass densities, ρ_{urn}, were measured based on Archimedes' principle with a micrometric balance and a density kit (Voyager® 610 GX, Ohaus Corporation, Florham Park, NJ, USA).

To estimate the mean acoustical parameters, V_{cavity}, α_{cavity}, of bone fragments without or with sand, the same methods were used on characteristic mixed samples, placed in the field of the transducers without separating interfaces. For the mass densities, ρ_{cavity}, several measurements were carried out on several different fragments, and the averages were calculated.

2.6. Rotational scanning

To study the behaviour of the algorithms in the face of variations in transducer positioning, each transducer was moved at different angles in its orthogonal plane around the urn, either with the electro-mechanical 2D-scanner using the 1MHz-transducer, or with the portable inspection unit using the 500kHz-transducer. Eight positions were tested with an angular step of 45°, and eight RF-signals were recorded with N = 4096 samples, for both configurations, 500 kHz and 1 MHz. For each RF-signal, the parametric identification algorithm was used to determine the geometrical and physical parameters of the urns.

2.7. Human-machine interface

A human-machine interface (Figure 11) has been finally developed to allow a non-specialist user to perform modelling process from a recorded RF-signal. This interface allows the user to choose different configurations (intermediate display, recording of the modelled signals) and to modify the processing parameters (variable depending on the material used), and provides the values of the geometrical and physical parameters of the urn.

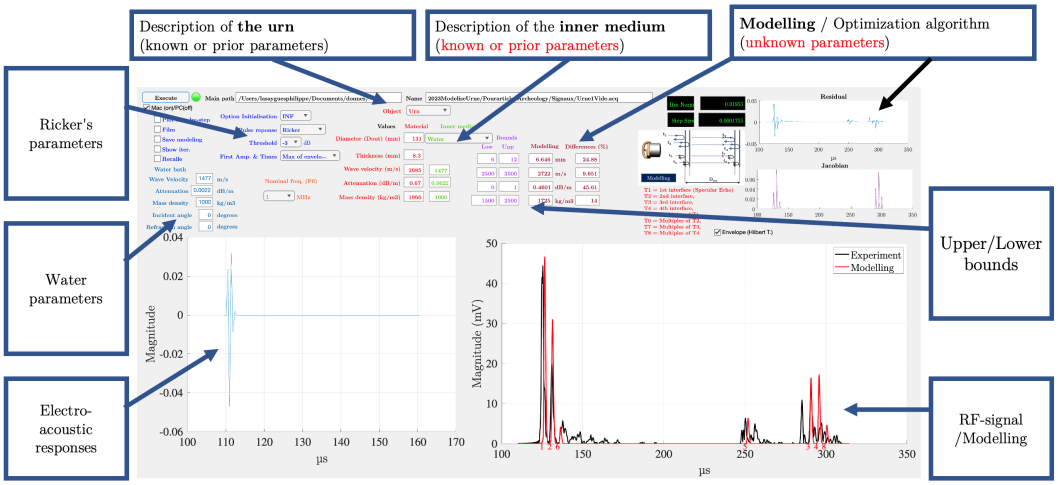

Figure 11: Human-machine interface for non-destructive testing of a funerary urn.

3. Results

3.1. Experimental RF-signals

Figures 12, 13, and 14 show the experimental recorded RF-signal at $y = 0°$ for the urn no1, no2 and no3 (inner cavity filled with water, water and bones, and water, bones and sand, respectively) when using the electro-mechanical 2D-scanner.

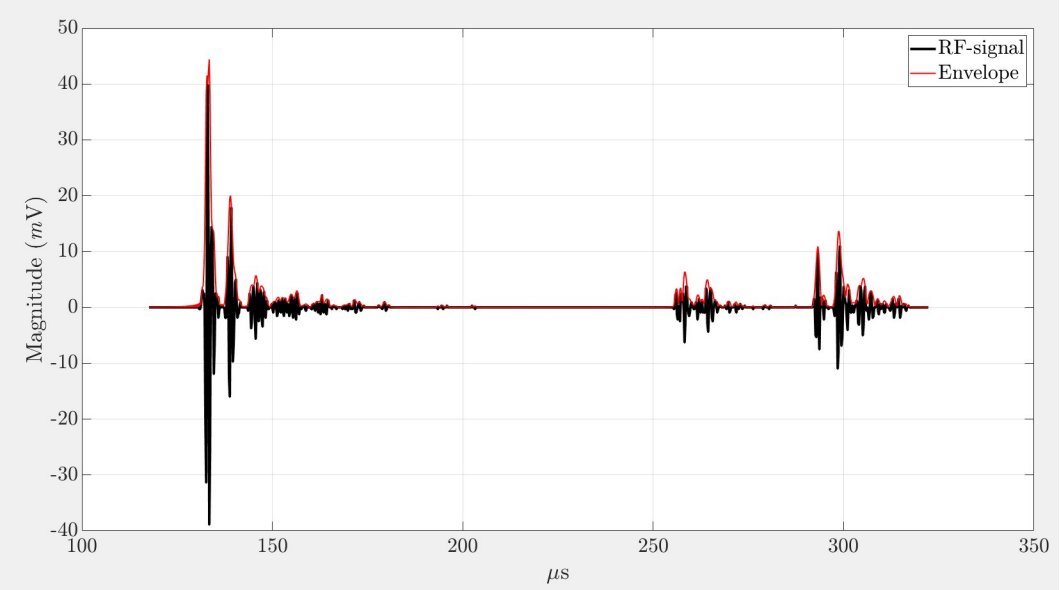

Figure 12: Temporal representation of the recorded RF-signal (black) and the envelope (red) for the artificial funerary urn no1 at $y = 0°$ (inner cavity filled with water). 1MHz configuration, scanner.

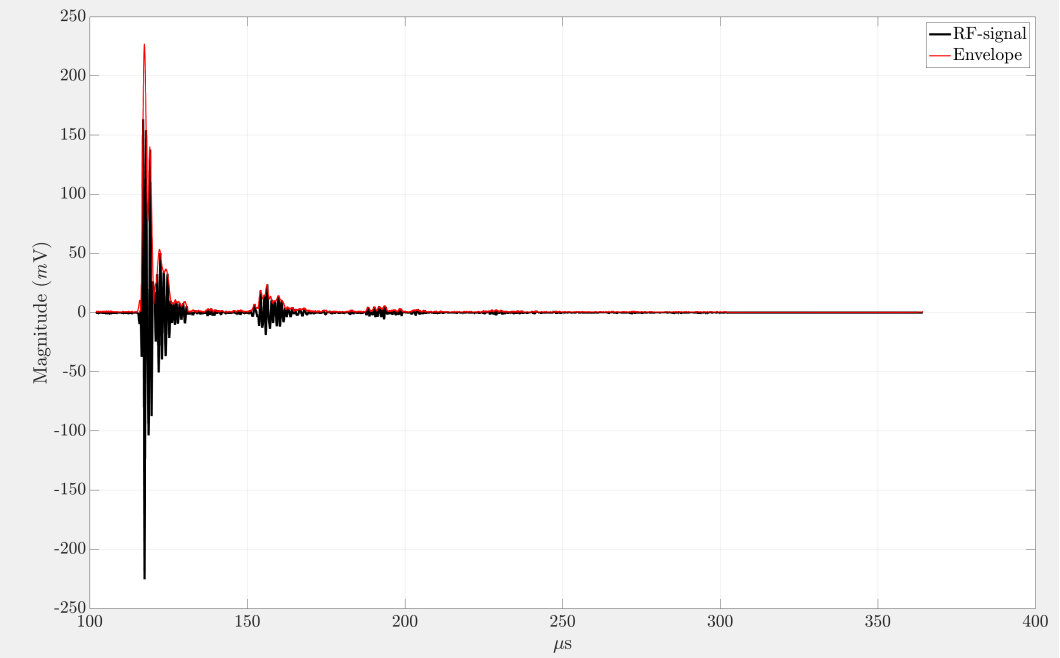

Figure 13: Temporal representation of the recorded RF-signal (black) and the envelope (red) for the artificial funerary urn no2 at $y = 0°$ (inner cavity filled with water and bones). 1MHz configuration, scanner.

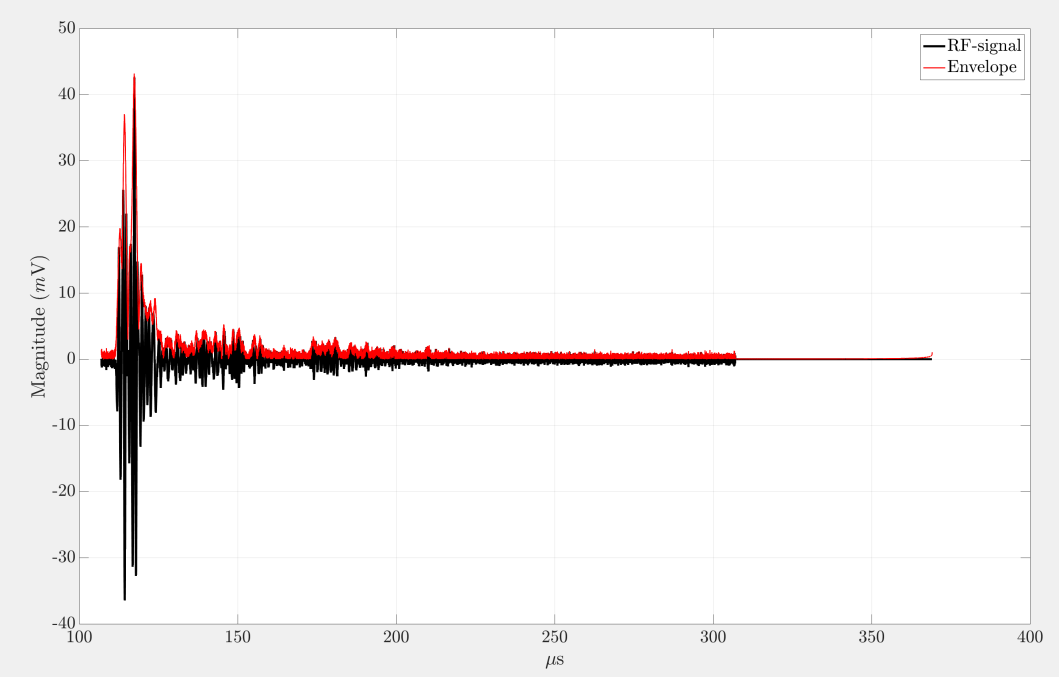

Figure 14: Temporal representation of the recorded RF-signal (black) and the envelope (red) for the artificial funerary urn no3 at $y = 0°$ (inner cavity filled with water, bones and sand). 1MHz configuration, scanner.

Figures 15, 16, and 17 show the experimental recorded RF-signal for the urn no1, no2 and no3 (inner cavity filled with water, water and bones, and water, bones and sand, respectively) when using the portable inspection unit (500kHz configuration).

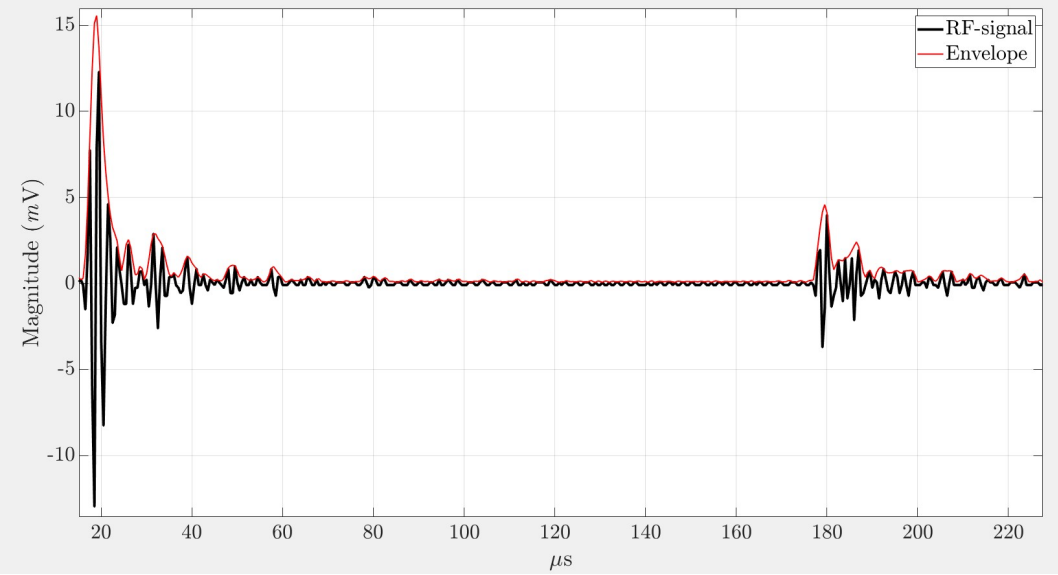

Figure 15: Temporal representation of the recorded RF-signal (black) and the envelope (red) for the artificial funerary urn no1 at $y = 0^\circ$ (inner cavity filled with water). 500kHz configuration, portable inspection unit.

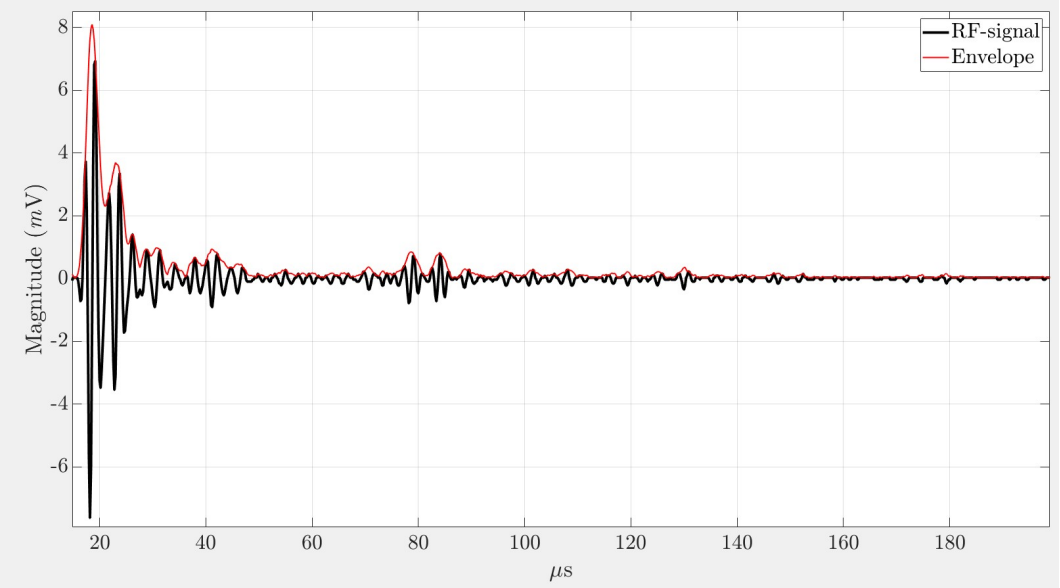

Figure 16: Temporal representation of the recorded RF-signal (black) and the envelope (red) for the artificial funerary urn no2 at $y = 0^\circ$ (inner cavity filled with water and bones). 500kHz configuration, portable inspection unit.

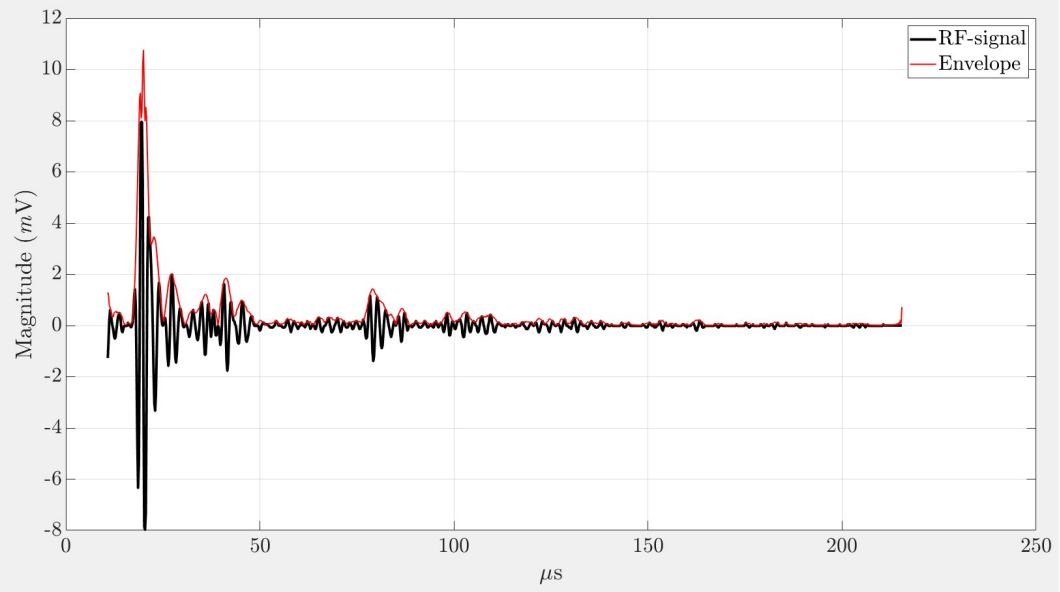

Figure 17: Temporal representation of the recorded RF-signal (black) and the envelope (red) for the artificial funerary urn no3 at $y = 0°$ (inner cavity filled with water, bones and sand). 500kHz configuration, portable inspection unit.

3.2. Prior parameters

Table 1 summarises the geometrical parameters of the three artificial funerary urns (measured with caliper).

Description	Units	Parameters	Values [Average±SD]
Urn no1			
Diameter	mm	D_{out}	129±0.2
Thickness	mm	E_{urn}	8.72±0.2
Urn no2			
Diameter	mm	D_{out}	131±0.2
Thickness	mm	E_{urn}	8.35±0.3
Urn no3			
Diameter	mm	D_{out}	131±0.3
Thickness	mm	E_{urn}	8.67±0.2

Table 1: Mean diameters and thicknesses measured with a caliper of the three artificial funerary urns for 10 positions around the urn.

Table 2 summarises the experimental physical parameters of the three clay pieces (Figure 2) from an urn constructed identically to those studied. For each parameter, 10 measurements were taken and the average values were used for the study.

Description	Units	Parameters	Values [Average±SD]
Sample no1			
US velocity[1]	m/s		3171±1.74
US attenuation (1 MHz)	dB/m		0.52±0.02
US attenuation (500 kHz)	dB/m		0.60±0.02
Mass density	kg/m^3		1993.1
Sample no2			
US velocity[1]	m/s		2717±1.3
US attenuation (1 MHz)	dB/m		0.70±0.01
US attenuation (500 kHz)	dB/m		0.59±0.02
Mass density	kg/m^3		1956.4
Sample no3			
US velocity[1]	m/s		3067±1.96
US attenuation (1 MHz)	dB/m		0.80±0.02
US attenuation (500 kHz)	dB/m		0.62±0.01
Mass density	kg/m^3		1949.9
Mean values[2]			
US velocity	m/s	V_{urn}	2985±238
US attenuation (1 MHz)	dB/m	α_{urn}	0.67±0.016
US attenuation (500 kHz)	dB/m	α_{urn}	0.60±0.011
Mass density	kg/m^3	ρ_{urn}	1966±23.29

[1] Mean value measured for 1 MHz and 500 kHz. [2]Mean values used to compare experiments and models for both 1MHz and 500kHz configurations.

Table 2: Experimental physical parameters measured for the three clay pieces by ultrasonic interferometry and Archimedes' principle.

Table 3 summarises the experimental *prior* parameters of the surrounding water, and of the media considered in the inner cavity. When the inner cavity was filled with water, the values considered were those of the water in the tank.

Description	Units	Parameters	Values [Average±SD]
Water			
Distance[1]	mm	H	86.5±0.4
Associated TOF	μs	t_1	117.36±0.5
US velocity	m/s	V_{water}	1480±5
US attenuation[2]	dB/m	α_{water}	0.0022
Mass density	kg/m^3	ρ_{water}	1000
Bones			
US velocity	m/s	V_{cavity}	3500
US attenuation (1 MHz)	dB/m	α_{cavity}	3
US attenuation (500 kHz)	dB/m	α_{cavity}	2
Mass density	kg/m^3	ρ_{cavity}	2000
Bones with sand			
US velocity	m/s	V_{cavity}	4200
US attenuation (1 MHz)	dB/m	α_{cavity}	3
US attenuation (500 kHz)	dB/m	α_{cavity}	2
Mass density	kg/m^3	ρ_{cavity}	1900

[1] Distances between the transducer and the urn (1MHz configuration, scanner). [2] Wave attenuation in water was assumed to be the same at 1 MHz and at 500 kHz.

Table 3: Experimental geometrical and physical parameters of the surrounding water, and of the media contained by the inner cavity.

3.3. Modelling of the wave propagation in a funerary urn

Figures 18 and 19 show the modelled impulse response, h_M, calculated with the experimental parameters for the urn no1 (using the mean parameters reported in Tables 1 and 2) at $y = 0°$, when the inner cavity was filled with water, and the convolution with the pseudo-Ricker wavelet (ie., the modelled signal $s(t)$, Eq. 5).

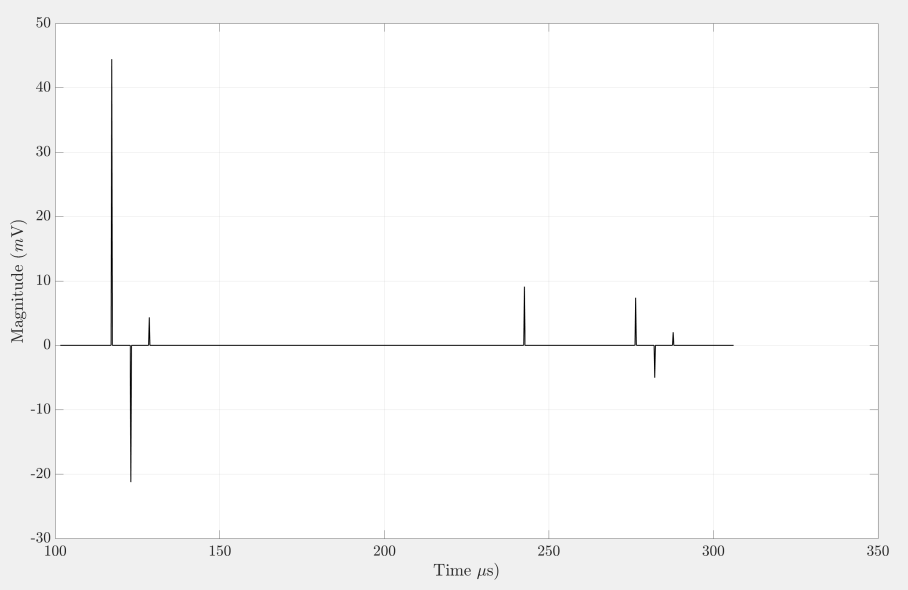

Figure 18: Temporal representation of the modelled impulse response, $h_M(t)$, calculated with the experimental parameters for the urn no1 at $y = 0°$, when the inner cavity was filled with water.

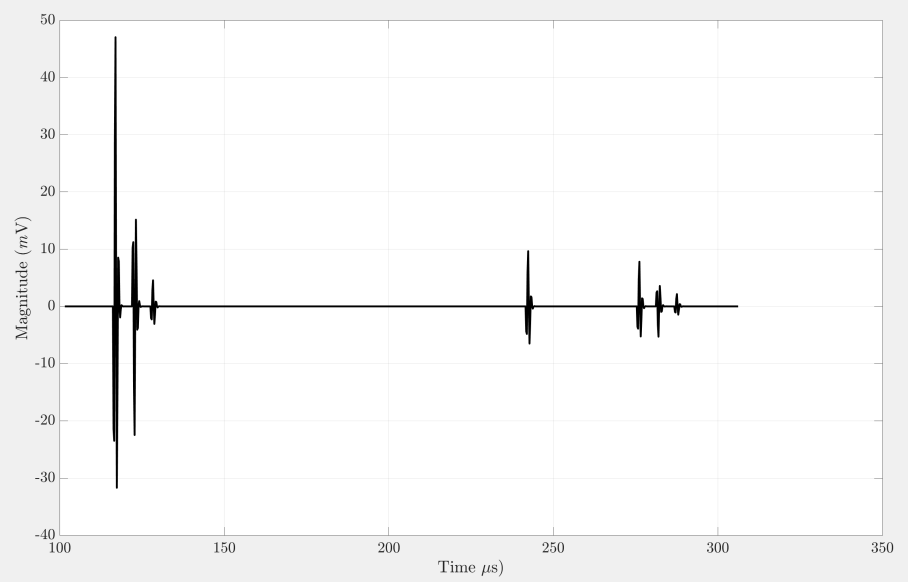

Figure 19: Temporal representation of the modelled signal, $s(t)$, calculated by the convolution of the pseudo-Ricker wavelet (1 MHz) and the modelled impulse response, $h_M(t)$.

3.4. Characterisation of the funerary urn

Tables 4 and 5 show the estimated geometrical and physical parameters of the three artificial funerary urns, and the lower and upper bounds chosen. The relative deviation expressed as a percentage (%) between the experimental and model parameters was defined by:

$$100 \times \frac{s_{mod}}{s_{mea}} - 1 \tag{17}$$

Parameters	Units	Bounds [Lower-Upper]	Experimental [Average]	Estimated [Modelled]	Deviations (Eq.17)
Urn no1	Empty				
E_{urn}	mm	[6-12]	8.72	8.73	0.11%
V_{urn}	m/s	[2000-3500]	2985	2983	0.07%
α_{urn} (1MHz)	dB/m	[0-1]	0.67	0.69	2.90%
ρ_{urn}	kg/m^3	[1500-2500]	1966	1966	0.01%
Urn no2	Bones				
E_{urn}	mm	[6-12]	8.35	8.55	2.34%
V_{urn}	m/s	[2000-3500]	2985	3037	1.71%
α_{urn} (1MHz)	dB/m	[0-1]	0.67	0.71	5.63%
ρ_{urn}	kg/m^3	[1500-2500]	1966	2019	2.63%
Urn no3	+sand				
E_{urn}	mm	[6-12]	8.67	9.01	3.77%
V_{urn}	m/s	[2000-3500]	2985	3224	7.41%
α_{urn} (1MHz)	dB/m	[0-1]	0.67	0.72	6.94%
ρ_{urn}	kg/m^3	[1500-2500]	1966	2110	6.82%

Table 4: Estimated geometrical and physical parameters of the three artificial funerary urns at $y = 0°$. 1MHz configuration, scanner

Parameters	Units	Bounds [Lower-Upper]	Experimental [Average]	Estimated [Modelled]	Deviations (Eq.17)
Urn no1	Empty				
E_{urn}	mm	[6-12]	8.72	8.70	0.23%
V_{urn}	m/s	[2000-3500]	2985	2990	0.17%
α_{urn} (500kHz)	dB/m	[0-1]	0.60	0.60	0.01%
ρ_{urn}	kg/m^3	[1500-2500]	1966	1965	0.05%
Urn no2	Bones				
E_{urn}	mm	[6-12]	8.35	8.45	1.18%
V_{urn}	m/s	[2000-3500]	2985	3025	1.32%
α_{urn} (500kHz)	dB/m	[0-1]	0.60	0.66	9.37%
ρ_{urn}	kg/m^3	[1500-2500]	1966	1987	1.06%
Urn no3	+sand				
E_{urn}	mm	[6-12]	8.67	8.98	3.45%
V_{urn}	m/s	[2000-3500]	2985	3035	1.65%
α_{urn} (500kHz)	dB/m	[0-1]	0.60	0.71	15.49%
ρ_{urn}	kg/m^3	[1500-2500]	1966	2200	10.64%

Table 5: Estimated geometrical and physical parameters of the three artificial funerary urns. 500kHz configuration, portable inspection unit.

The acceptability criterion was defined so that the difference between the experimental and model parameters was less than 10^{-5}. Under these conditions, the total number of iterations was 14 for the parameters estimated from the modelled signals for urns 1 and 2, and 12 for urn 3. The computation time was 1 sec per iteration. The convergence of the algorithm in all the trials of this work did not exceed 15 seconds.

Figure 20 shows steps 1, 2, 3, 4, 7 and 14 (the final one) for urn no1 at $y = 0°$ (inner cavity filled with water), for geometrical parameters given in Table 1, and the mean physical parameters given in Tables 2 and 3.

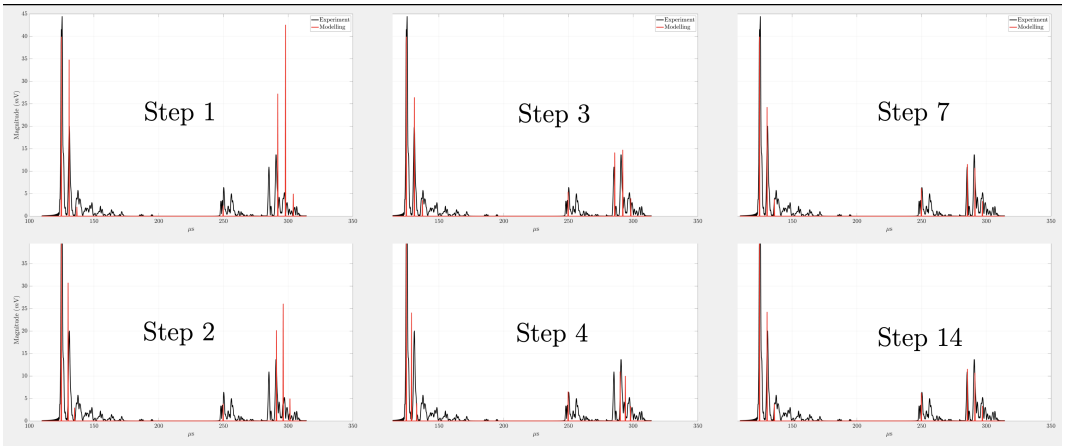

Figure 20: Temporal representation of the envelopes of the experimental RF-signal (black) obtained for the urn no1 and of the modelled response, h_M, obtained by the algorithm at iterations no1, 2, 3, 4, 7, and 14 (red). 1MHz configuration, scanner

The final results, (i.e., the modelled signal $s(t)$) are presented in Figure 21 for the 1MHz-configuration (scanner), and in Figure 22 for the 500kHz-configuration (portable inspection unit).

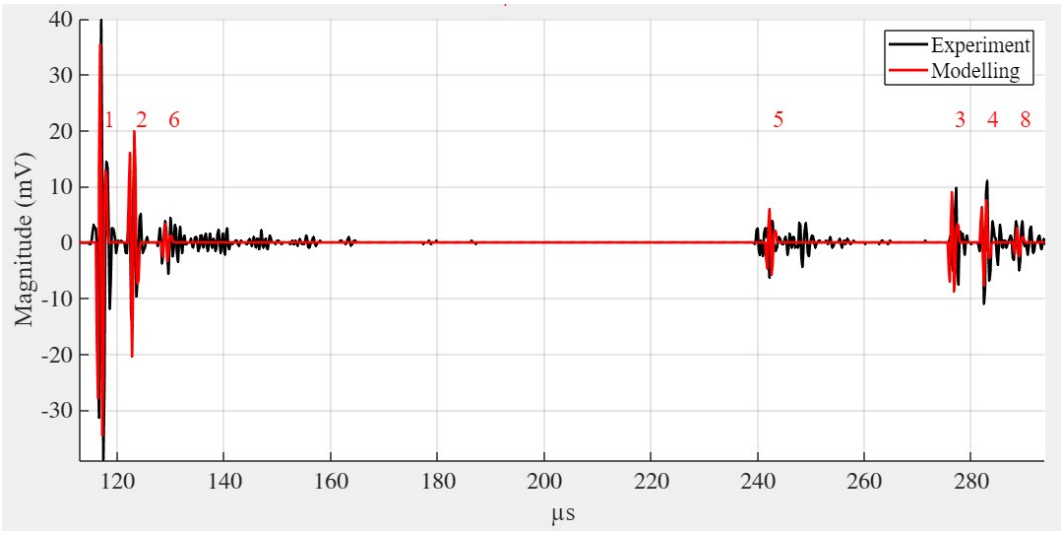

Figure 21: Temporal representation of the experimental recorded RF-signal (black) and the modelled signal, $s(t)$, (red) for the artificial funerary urn no1 at $y = 0°$ (inner cavity filled with water). 1MHz configuration, scanner.

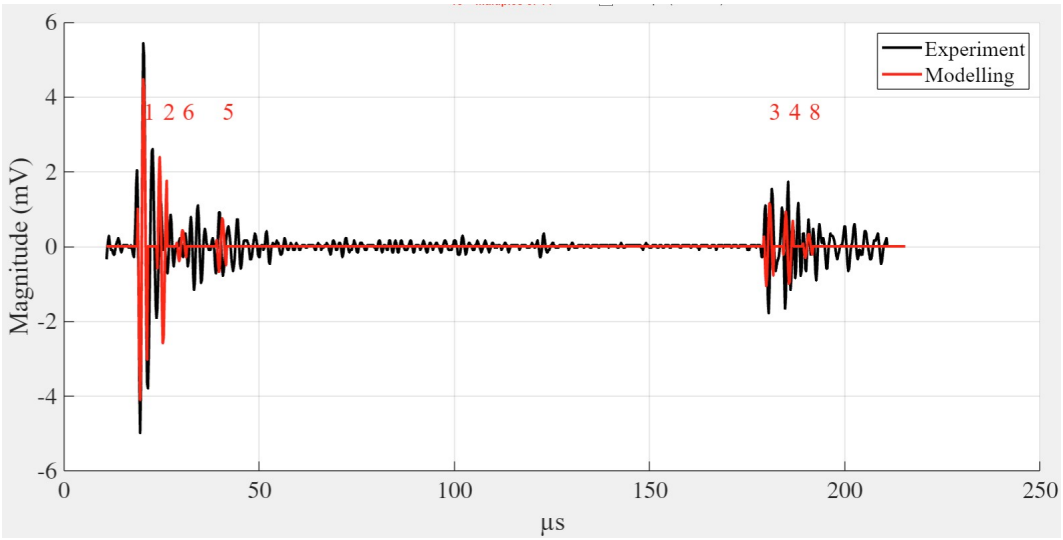

Figure 22: Temporal representation of the experimental recorded RF-signal (black) and the modelled signal, $s(t)$, (red) for the artificial funerary urn no1, (inner cavity filled with water). 500kHz configuration, portable inspection unit

The numbers (in red) in the figures correspond to the different TOF (Figure 9). Figures 23, 24, 25 and 26 show the temporal representations of the experimental RF-signals obtained for the artificial funerary urns when the inner cavity was filled respectively with water and bones (urn no2), and water, bones and sand (urn no3), and the corresponding modelled signals, for 1MHz-configuration (scanner), and the 500kHz-configuration (portable inspection unit). In these cases, the physical parameters for the inner cavity were those of the bones, without and with sand (Table 3).

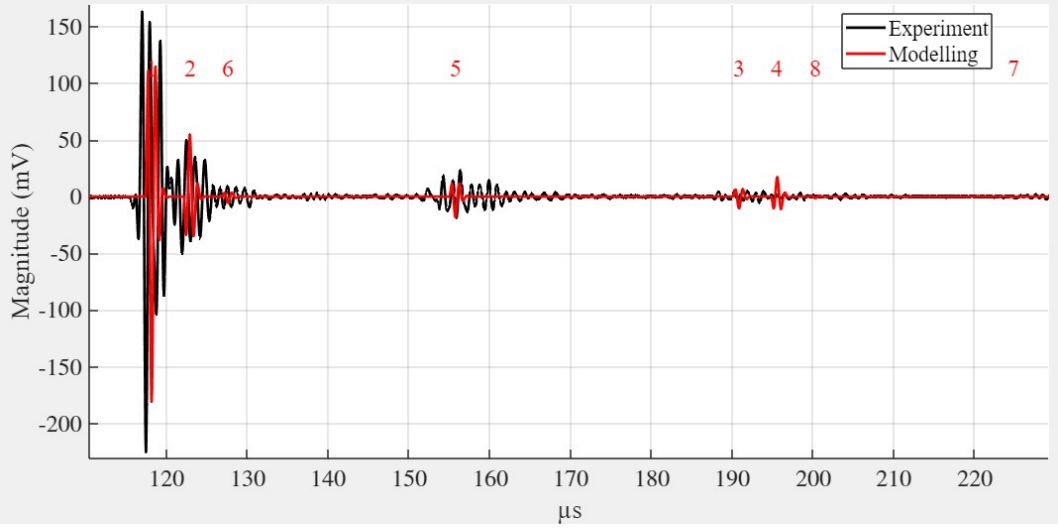

Figure 23: Temporal representation of the experimental recorded RF-signal (black) and the modelled signal, $s(t)$, (red) for the artificial funerary urn no2 at $y = 0°$ (inner cavity filled with water and bones). 1MHz configuration, scanner.

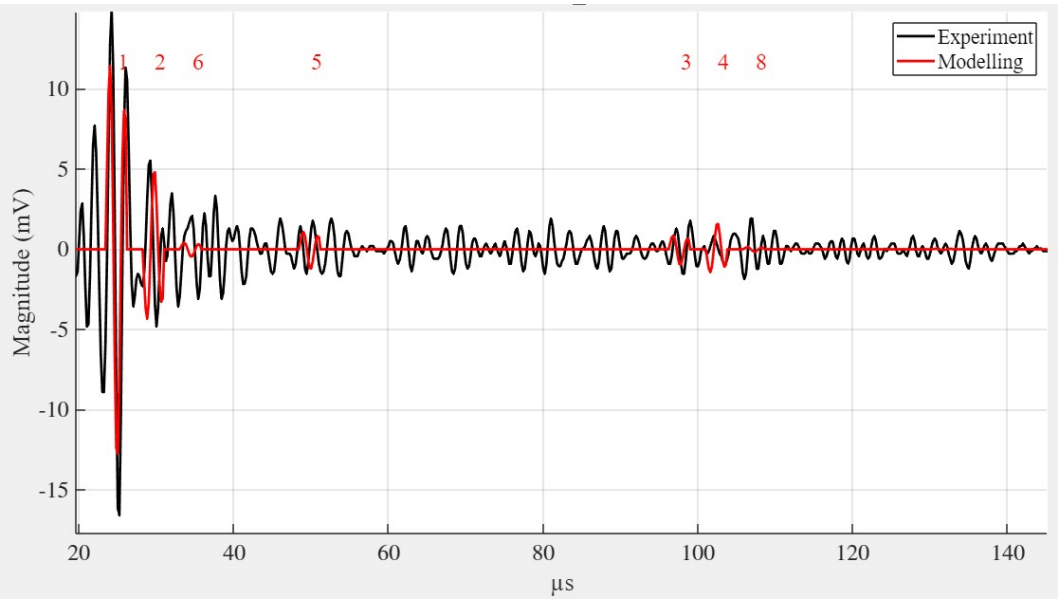

Figure 24: Temporal representation of the experimental recorded RF-signal (black) and the modelled signal, $s(t)$, (red) for the artificial funerary urn no2 (inner cavity filled with water and bones). 500kHz configuration, portable inspection unit.

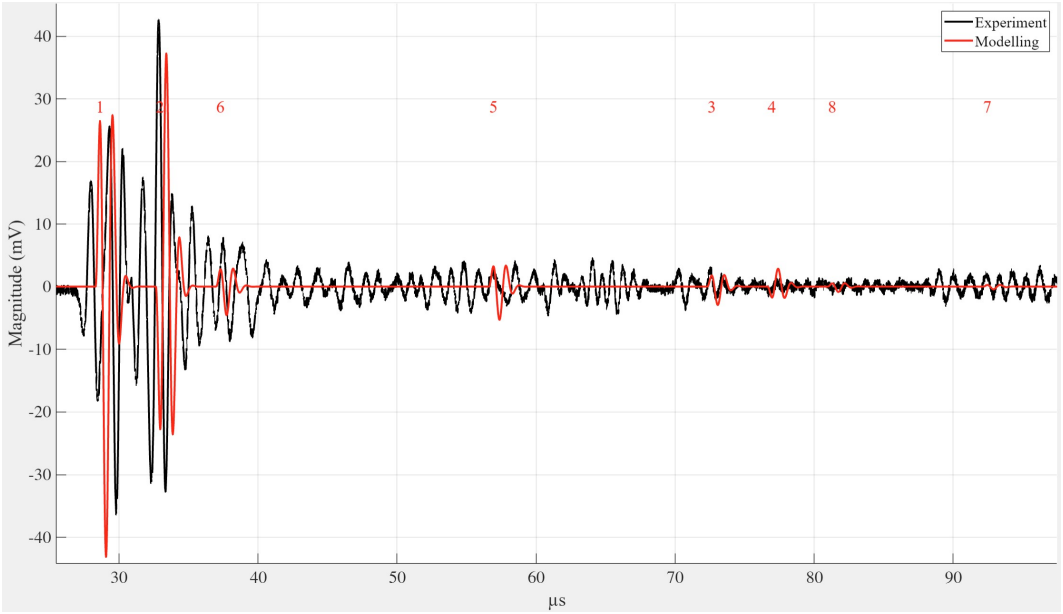

Figure 25: Temporal representation of the experimental recorded RF-signal (black) and the modelled signal, $s(t)$, (red) for the artificial funerary urn no3 at $y = 0°$ (inner cavity filled with water, bones and sand). 1MHz configuration, scanner.

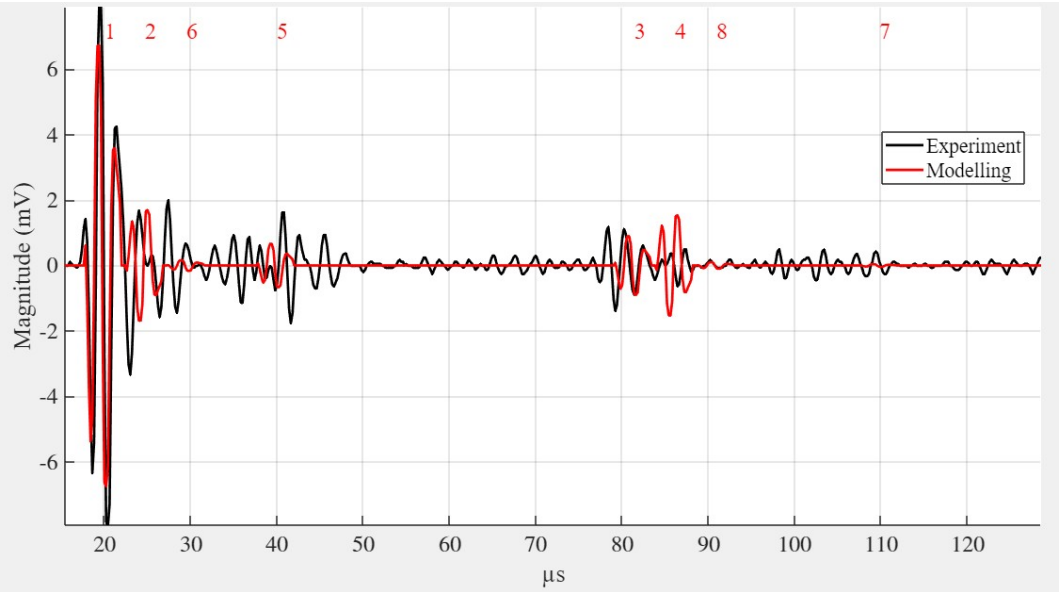

Figure 26: Temporal representation of the experimental recorded RF-signal (black) and the modelled signal, $s(t)$, (red) for the artificial funerary urn no3 (inner cavity filled with water, bones and sand). 500kHz configuration, portable inspection unit.

3.5. Rotational scanning

Figures 27 and 28 show the model parameters of the artificial funerary urns, when the inner cavity was filled with water (no1), with water and bones (no2), and with water, bones and sand (no3), for 8 positions over 360° and both experimental configurations.

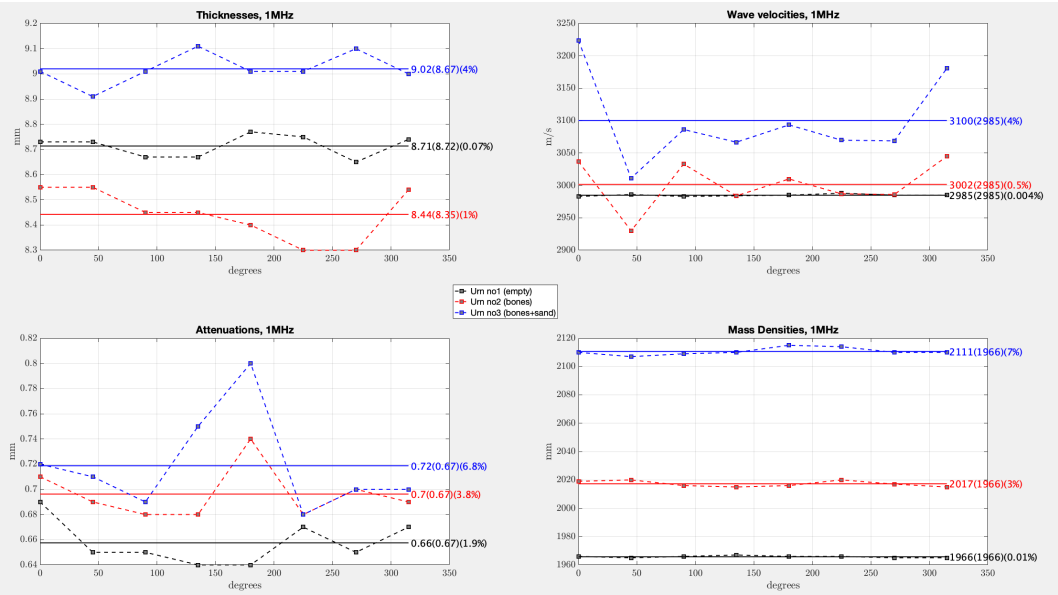

Figure 27: Angular parametric study of the urns. The symbols represent the values per angle for the urns, when the inner cavity was filled with water (black), water and bones (red), and water, bones and sand (blue). The solid line corresponds to the average of the parameters. The mean parameter is shown on the right, along with the reference and deviation (percentage) values. 1MHz configuration, scanner.

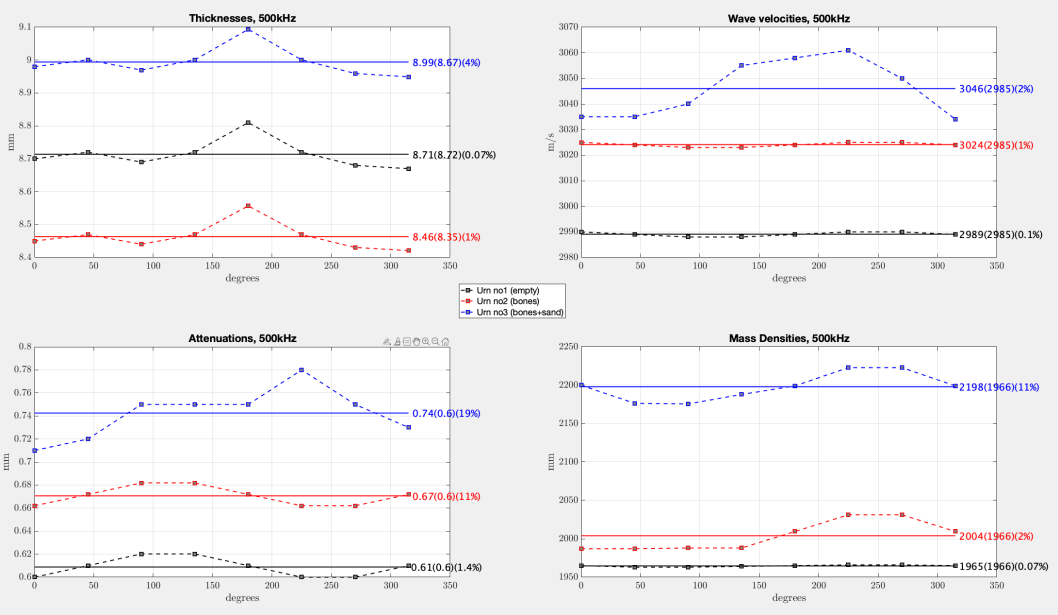

Figure 28: Angular parametric study of the urns. The symbols represent the values per angle for the urns, when the inner cavity was filled with water (black), water and bones (red), and water, bones and sand (blue). The solid line corresponds to the average of the parameters. The mean parameter is shown on the right, along with the reference and deviation (percentage) values. 500kHz configuration, portable inspection unit.

Tables 6 and 7 show the mean parameters of the artificial funerary urns for 8 angles of incidence over 360°, for both experimental configurations.

Parameters	Units	Experimental [Average]	Estimated [Average±SD]	Deviations (Eq.17)
Urn no1	Empty			
E_{urn}	mm	8.72	8.71±0.04	0.07%
V_{urn}	m/s	2985	2985±1.5	0.02%
α_{urn} (1MHz)	dB/m	0.67	0.66±0.02	1.9%
ρ_{urn}	kg/m^3	1966	1966±0.7	0.01%
Urn no2	Bones			
E_{urn}	mm	8.35	8.44±0.1	1.1%
V_{urn}	m/s	2985	3002±35.5	0.55%
α_{urn} (1MHz)	dB/m	0.67	0.7±0.02	3.77%
ρ_{urn}	kg/m^3	1966	2017±2	2.54%
Urn no3	+sand			
E_{urn}	mm	8.67	9.02±0.06	3.88%
V_{urn}	m/s	2985	3100±64.2	3.71%
α_{urn} (1MHz)	dB/m	0.67	0.72±0.04	6.78%
ρ_{urn}	kg/m^3	1966	2111±2.4	6.85%

Table 6: Estimation of the parameters of an artificial funerary urn for 8 angles of incidence over 360°. 1MHz configuration, scanner.

Parameters	Units	Experimental [Average]	Estimated [Average±SD]	Deviations (Eq.17)
Urn no1	Empty			
E_{urn}	mm	8.72	8.71± 0	0.07%
V_{urn}	m/s	2985	2989±0.8	0.14%
α_{urn} (500kHz)	dB/m	0.60	0.61±0.01	1.44%
ρ_{urn}	kg/m^3	1966	1965±1.1	0.07%
Urn no2	Bones			
E_{urn}	mm	8.35	8.46±0	1.34%
V_{urn}	m/s	2985	3024±0.8	1.29%
α_{urn} (500kHz)	dB/m	0.60	0.67±0.01	10.53%
ρ_{urn}	kg/m^3	1966	2004±18.2	1.89%
Urn no3	+sand			
E_{urn}	mm	8.67	8.99±0	3.6%
V_{urn}	m/s	2985	3046±10.5	2.0%
α_{urn} (500kHz)	dB/m	0.60	0.74±0.02	19.19%
ρ_{urn}	kg/m^3	1966	2198±17	10.56%

Table 7: Estimation of the parameters of an artificial funerary urn for 8 angles of incidence over 360°. 500kHz configuration, portable inspection unit.

4. Discussion

In this paragraph, we will discuss the results and their interpretation from the point of view of the modelling assumptions, as well as from the point of view of the *in situ* non-destructive testing of ancient funerary urns. Future research directions will also be highlighted.

4.1. Presence of water in the urn

What needs to be observed in our study is the presence of water in the urns in our study. Whatever the experimental device, the urns are always filled with water, to allow the ultrasonic waves (at the frequencies considered, 500 kHz and 1 MHz) to propagate with low variations in attenuation (<1 dB/m). This is obviously a very important limitation of this study, as the urns found at archaeological excavation sites are not (necessarily) filled with water. However, it is important to know that ultrasounds can also be propagated through the air. This is a special technology that will have to be tested in future experiments. There have been major technical advances in this field, [14].

4.2. Study of RF- and modelled signals

The signals for a cavity containing water, water and bones, and water, bones and sand, are different and more or less noisy; signal-to-noise ratio between 3 dB (water, bones and sand) to 15 dB (water only). The first echo (t_1) on the first water/urn interface (whatever the urn) has a higher dynamic range than the other wave packets that follow (t_2 to t_8). This is due to the acoustical impedance contrast between the water and the clay. The acoustical impedance of the clay (≈ 6 MRays) is greater than that of the water (≈ 1.5 MRays), and the reflection coefficient (Eq. 11) between the two media is high (≈ 0.7). The acoustical intensity of the waves transmitted into the urn is therefore greatly reduced. Conversely, the waves reflected in the inner cavity do not lose too much energy.

Despite all the variations in acoustical intensity, the wave packets are fairly well identifiable, although in the case of urn no3 (water, bone and sand), the signal-to-noise ratio is low, and the wave packets more difficult to identify. With regard to this last point, the benefits of the model are significant. The wave packets are identified on the modelled signals, enabling the corresponding wave packets to be identified on the RF-signals by superposition whatever the signal-to-noise ratio.

In the case of an empty urn (i.e. filled with water only), the TOF t_7 does not appear. This TOF corresponded to the second reflection inside the inner cavity. The wave velocity being that of the waves in water, it was slower than in the wall of the urn, and the TOF was longer, and higher than the recording time of the RF-signals. For urns containing bones and/or sand, the waves were accelerated (and attenuated) in the inner cavity because the acoustical parameters were higher than those of water alone, and then the multiple echoes arrived early enough to be recorded.

4.3. Relevance of the analytical parametric model

To define the analytical parametric model composed of four interfaces, a number of hypotheses were introduced, not all of which had the same impact on the model of the signals. The chosen number of back-and-forth travels (equal to 2) was well suited. For the empty urn, it would be possible to increase the number of back-and-forth travels (and therefore the number of TOF), but some of these TOF would be outside the time limits of the recorded signals, and therefore unusable. The empty urn was not the main objective of the study and there is no interest in modifying the recording times or increasing the number of points, which would result in longer processing times. With bones and sand (a more realistic

archaeological condition), all the TOF would be closer together (the wave velocities increase), but as attenuation would be greater, the wave packets would not be distinguished from the noise. Adding back-and-forth travels and TOF to the model would also introduce a bias which would add processing time. In fact, the parametric identification algorithm would then have more difficulty in converging quickly. Tests were carried out which confirmed these remarks.

Ray theory was adopted for this modelling process. This means that the incident wave is symbolised by a straight ray perpendicular to the interface. This assumption is valid at high frequencies, i.e. short wavelengths compared with the thickness and diameter of the urn (Table 8). The higher the frequency, the greater the number per wavelength, and the more valid this high-frequency assumption. Wave packets on 1MHz signals are better resolved (i.e. visible), but noisier, whereas 500kHz signals are less noisy, but the wave packets are harder to identify. For non-destructive testing to be extended to other archaeological objects, such as urns from different periods, pottery or vases, and for this high-frequency hypothesis to be plausible, the frequency (and the wavelength) of the transducers used will have to be adapted to the dimensions/thickness of the objects.

The calculated deviations (Tables 6 and 7) between the estimated and experimental parameters, at several points around the urns, are greater at 500 kHz than 1 MHz, particularly for the urns containing bones, especially for the attenuation measurements. This is also due to the lower resolution of the signals at low frequencies. This can be seen in Figures 22, 24 and 26. The superposition of the RF and modelled signals is correct for TOF, but less good for amplitudes, particularly for t_6, or t_7.

	Units	Water	Water	Urn	Urn
Wave velocity	m/s	1480	1480	2985	2985
Frequency	MHz	0.5	1	0.5	1
Wavelength (λ)	mm	≈ 3	≈ 1.5	≈ 6	≈ 3
Thickness E_{urn}	mm	≈ 8.6	≈ 8.6	≈ 8.6	≈ 8.6
Number of λ		≈ 3	≈ 6	≈ 1.5	≈ 3
Diameter D_{out}	mm	≈ 130	≈ 130	≈ 130	≈ 130
Number of λ		≈ 43.3	≈ 86.6	≈ 21	≈ 43.3

Table 8: Values used for high-frequency approximation.

Shear waves were neglected in this work, considering that their attenuation

was very strong in the clay the urns were made of, but also that the incidence of the transmitted wave was very precisely normal to the water/urn interface. This hypothesis is discussed. At a distance of H = 86.5 mm, the angular aperture of the ultrasonic beam from the 1MHz-transducer is less than 3°. As the radius of curvature of the urn was much larger, the wavefront and the water/urn interfaces were considered to be parallel, so that any mode conversion (compression to shear waves, and vice versa) was highly negligible compared with the refraction of compression waves. For the 500kHz-transducer, the mode conversion problem did not arise because the transducer was placed in contact with the urn, with an angular aperture of 2°. There was therefore no propagation of shear waves in the urn. It should also be noted that the critical angle for compression waves, $sin^{-1}(V_{\text{water}}/V_{\text{urn}})$, is 30°. Beyond this angle of incidence, no more compression waves propagate. This angle could be exceeded in the experiments carried out in this study.

Also, a layer of clay is about 20 mm high, so the focal area (16 mm^2) can cover one or two layers. From one layer to the next, the acoustical properties of the clay may vary slightly. This explains why the estimated and the experimental values differ with deviations lower than 10%. This also explains the additional wave packets that appear in the RF-signals (most pronounced at 1 MHz) after the TOF (t_5) and (t_6), and that do not appear in the analytical parametricmodel, as they are not taken into account deliberately. Numerical modelling process, using finite-element modelling for example, makes it possible to add these physical considerations to the model, and to highlight multiple propagation phenomena difficult to understand. But they have first nothing to add to the objective of the identification of urns containing or not containing bones. And, second, they would add difficulties and constraints (the equations for calculating the times (Eqs. 8, 9 and 10) would be different), and, consequently, the processing time would increase which, for *in situ* use, would not be relevant.

The strongest assumptions made on the analytical parametric model concern the physical parameters (wave velocity and attenuation, mass density) used as *known* (*prior*) information, and considered to be homogeneous and identical for all the urns. Even if the urns were made by the same specialist, they would contain intra-urn differences. Those intra-urn differences surely also existed in ancient urns. The acoustical parameters measured in the clay (used to define the bounds of the optimisation algorithm) were of the same order of magnitude but there were differences between the 3 small samples. The standard deviation is 238 m/s for the velocities, which is significant and shows that the assumption of homogeneity of the clay and the urn can be questioned. There are therefore inter-urn differences,

which was expected, but also intra-urn differences, which can be significant. In the context of an *in situ* NDT procedure, the parametric information on the objects will not be known. It will be necessary to have information about the material (type of clay or ceramic, or object material) or to increase the values of the lower and upper bounds of the algorithm, thus increasing the processing time.

The parametric values, as well as the deviations between the experimental and estimated parameters, are larger when the urn was filled with water, bone and sand, and become smaller when only water was present. Similarly, the standard deviations are greater for full urns than for empty urns, and for all parameters except mass density. This can be explained by the fact that with bones and sand/or no sand, the waves were more strongly attenuated (2-3 dB/m) in the inner cavity because of multiple diffraction phenomena and/or intrinsic absorption. The bones diffracted the waves in the inner cavity in all spatial directions, and the sand absorbed a large proportion of the acoustical intensity. The reflected waves (those returning to the transducer) had less energy. The wave packets were less distinguishable from the surrounding noise, and the analytical parametric model had difficulty finding the 2nd order TOF (t_5 to t_8).

The values of the physical parameters of bone and sand also need to be discussed. Laboratory measurements of velocity, attenuation and mass density carried out on "characteristic mixtures" of bones and of sand cannot be generalised, although these mean values (*in situ*) should always be of the same order of magnitude. The values measured do not take into account the type of bone - there are very large differences between cortical and porous bone - or the density (compactness) of the mixture of fragmentary bones, which increases still further in the presence of sand. If the bones are all porous and the sand not very compact, the wave velocities and attenuations will be lower (close to what they would be if they were propagated in water) than for a mixture of cortical bone and very compact sand.

4.4. Reproducibility and resistance of the parametric identification algorithm

The optimisation algorithm based on the Levenberg-Marquardt method is well suited to the task of identifying the geometrical and physical parameters of a funerary urn, and detecting the presence or absence of bone inside it. It is fast (a few seconds), and accurate (deviations $< 10\%$). However, when the urn contains bones and sand, the algorithm converges with greater difficulty (greater error) on the TOF of the third and fourth interfaces, and remains focused on the first two, with greater signal-to-noise ratio (lower noise). For bone-containing urn, the errors were higher, since the minimisation algorithm sought the same number of

variables, for the same threshold (10^{-5}), but could converge on several minima, reach the upper bounds, and ultimately find no solution, or a false solution. The Levenberg-Marquardt algorithm is less well-suited to very noisy signals, but is still suitable for our study.

With the rotational study, the algorithm was tested for reproducibility and resistance. Values at 500 kHz are more homogeneous and standard deviations lower for all parameters. Low-frequency signals are less well resolved than those obtained at 1 MHz. Errors are greater in relation to the same reference, but conversely, the signals are very similar and less sensitive to position, and therefore to variations in the urn, than those at 1 MHz. The algorithm is highly resistant to variations, and the lower the frequency, the greater the reproducibility.

There are also problems related only to numerical algorithms. For example is the strong non-linearity of the cost function C (Eq. 16) makes the gradient-based minimisation algorithms only converge to the solution if they are started close to the global minimum, i.e., provided that the initial model is already of good "quality" (low parameter bias). We know that, in this analytical and numerical form, the proposed algorithm has application limits. We have to admit that it will make mistakes, unless two possible ways are forwarded. Firstly, the linear propagation assumption could be revised, and more complex and time-consuming non-linear algorithms introduced, such as the full waveform inversion method, [15]. Secondly, it would be possible to use commercial (or home-made) software, which can be expensive, and would increase processing time. This is not desirable.

5. Conclusions

The aim of this work was to study the feasibility of non-destructive ultrasonic testing of ancient funerary urns. More specifically, the aim was to propose a method for identifying the geometrical and physical parameters of an urn, and detecting the presence or absence of bone inside it.

Firstly, an analytical model based on assumptions and approximations relating to ultrasonic wave propagation in urns was proposed. This mathematical model is based on the convolution of a series of Dirac distributions, which models the impulse response of the propagating medium, by a pseudo-Ricker wavelet, which models the impulse response of the ultrasonic device. The Dirac distribution series is representative of homogeneous propagation of compression waves only, in an isotropic, weakly dispersive medium. The pseudo-Ricker wavelet is representative of linear and causal electro-acoustics. This model represents wave/urn interaction phenomena very well when the urn is filled with water. It remains

valid when the urn contains bones, or bones and sand. Although slightly biased, it correctly detects the presence or absence of bone fragments. However, it does not allow us to discriminate between buried and burnt bones, the nature of the fragments (trabecular or cortical), or the quantity of bone contained in the urn. Several improvements need to be considered.

The model is limited to four parameters that only concern the urn: urn thickness, wave velocity and attenuation in the clay, and clay mass density. Propagation in the inner cavity, which is assumed to be known in this study, should be introduced into the model, wave/bone interaction phenomena should be taken into account, and the number of variables should be increased to seven, with the addition of bone and sand velocities, attenuations and mass densities.

The parametric identification algorithm, based on the minimisation of a functional between a measure and a model, is effective for four variables, and enables us to correctly identify a funerary urn and detect the presence or absence of bone inside it. Deviations between experimental and estimated parameters do not exceed 10%, which is acceptable. Convergence, computation time, resilience and, more generally, the benefit/performance ratio are very favourable to *in situ* use. Adapted to the linear modelling process, limited to the wave/urn interaction phenomena alone, the processing time is less than 15 seconds on average (a few minutes for a complete examination) with a result that enables a specialist to compare two urns with each other. But we would have to test other configurations, other materials, without any *known or prior* information, and adapt it to a seven-variable modelling process. This would require a paradigm shift from a linear to a non-linear approach. Modelling process would be more complex, requiring more in-depth numerical notions. Processing times would increase sharply, and the benefit/performance ratio would have to be discussed, particularly in relation to the precision expected by archaeologists and ceramists.

From our point of view, it would be preferable to keep on with linear modelling process, which is simpler and faster, and work on AI algorithms (deep learning, for example) that could take into account the model's imperfections and deviations, and enable us to establish a classification of the materials used for ancient funerary urns; different clays or materials, different types of manufacturing process, different shapes; and discriminate the nature of the inner cavity.

Declaration of Competing Interest

The authors declare no conflict of interest. The funders had no role in the design of the study; in the collection, analysis, or interpretation of the data; in the

writing of the manuscript, or in the decision to publish the results.

Acknowledgments

The authors thank Jeanne Baldisser from the school of engineering ”Centrale Méditerranée” for her work while she was an intern in our laboratory.

Funding

The project leading to this publication has received funding from the Excellence Initiative of Aix-Marseille University - A*Midex, a French “Investissements d’Avenir programme” - Institut d’archéologie méditerranéenne (ARKAIA, AMX-19-IET-003), and Institut Mécanique et Ingénierie (IMI, AMX-19-IET-010). Elise Doveri’s PhD thesis was funded by the French Ministry of Research and Matthieu Boutoille’s internship was funded by the Laboratory of Mechanics and Acoustics, CNRS.

References

[1] G. Giacobini, Richesse et diversité du rituel funéraire au paléolithique supérieur: L’exemple des sépultures italiennes, Diogène 214 (2) (2006) 24. doi:10.3917/dio.214.0024.
URL http://www.cairn.info/revue-diogene-2006-2-page-24.htm

[2] P. Bailet, P. Georges, C. Arlaud, La crémation hellénistique et romaine à Alexandrie (Égypte). De la fouille des urnes à la restitution des pratiques funéraires, 2020.
URL https://hal.archives-ouvertes.fr/hal-02111712

[3] C. Bernand, Éric Crubézy, Aux origines des rites funéraires. Voir, cacher, sacraliser: Paris, Odile Jacob, 2019, 253 p., Archives de sciences sociales des religions (192) (2020) 179–180. doi:10.4000/assr.57407.
URL http://journals.openedition.org/assr/57407

[4] A. Richier, L’incidence des réceptacles funéraires sur la position et la décomposition des cadavres : étude de cas archéologiques modernes et contemporains, Bulletins et Mémoires de la Société d’Anthropologie de Paris 32 (1-2) (2020) 59–74. doi:10.3166/bmsap-2020-0070.

URL https://bmsap.revuesonline.com/10.3166/bmsap-2020-0070

[5] G. (France), S. d. Larminat, R. Corbineau, Y. Gleize, A. Corrochano, J. Soulat (Eds.), Rencontre autour de nouvelles approches de l'archéologie funéraire: actes de la 6e Rencontre du Gaaf à Paris, Institut national d'histoire de l'art, les 4 et 5 avril 2014, no. no 6 in Publication du Gaaf, Groupe d'anthropologie et d'archéologie funéraire, Reugny, 2017, oCLC: on1112170177.

[6] L. Harvig, N. Lynnerup, J. A. Ebsen, COMPUTED TOMOGRAPHY AND COMPUTED RADIOGRAPHY OF LATE BRONZE AGE CREMATION URNS FROM DENMARK: AN INTERDISCIPLINARY ATTEMPT TO DEVELOP METHODS APPLIED IN BIOARCHAEOLOGICAL CREMATION RESEARCH: Computed tomography and radiography of urns from Denmark, Archaeometry 54 (2) (2012) 369–387. doi:10.1111/j.1475-4754.2011.00629.x.
URL https://onlinelibrary.wiley.com/doi/10.1111/j.1475-4754.2011.00629.x

[7] I. Le Goff, Nouvelles technologies numériques, nouveau regard porté sur les crémationsPublisher: Inrap (Jun. 2018). doi:10.34692/74QM-S229.
URL https://sstinrap.hypotheses.org/856

[8] M. L. Puil-Texier, L'application de l'examen tomodensitométrique aux dépôts de crémation: Une reconsidération des méthodes d'investigation, Les Nouvelles de l'archéologie (159) (2020) 31–35. doi:10.4000/nda.9202.
URL http://journals.openedition.org/nda/9202

[9] K. Kiss, C. Libor, Paleoradiological tests in Hungary and abroad, Hungarian Archaeology 11 (1) (2022) 8–15. doi:10.36338/ha.2022.1.3.
URL http://files.archaeolingua.hu/2022TA/Upload/Kiss-Libor_E22TA.pdf

[10] P. Laugier, Q. Grimal (Eds.), Bone Quantitative Ultrasound: New Horizons, Vol. 1364 of Advances in Experimental Medicine and Biology, Springer International Publishing, Cham, 2022. doi:10.1007/978-3-030-91979-5.

URL https://link.springer.com/10.1007/978-3-030-91979-5

[11] P. Lasaygues, Ultrasonic discrimination and modelling for crack-tip echoes, Nondestructive Testing and Evaluation 26 (1) (2011) 67–85. doi:10.1080/10589759.2010.497840.
URL http://www.tandfonline.com/doi/abs/10.1080/10589759.2010.497840

[12] E. Vasanelli, D. Colangiuli, A. Calia, M. Sileo, M. A. Aiello, Ultrasonic pulse velocity for the evaluation of physical and mechanical properties of a highly porous building limestone, Ultrasonics 60 (2015) 33–40. doi:10.1016/j.ultras.2015.02.010.
URL https://linkinghub.elsevier.com/retrieve/pii/S0041624X15000438

[13] P. Lasaygues, A. Arciniegas, L. Espinosa, F. Prieto, L. Brancheriau, Accuracy of coded excitation methods for measuring the time of flight: Application to ultrasonic characterization of wood samples, Ultrasonics 89 (2018) 178–186, wOS:000436496200019. doi:10.1016/j.ultras.2018.04.013.

[14] F02 Committee, Test Method for Evaluation of Seal Quality and Integrity Using Airborne Ultrasound, Tech. rep., ASTM International. doi:10.1520/F3004-13R20.
URL http://www.astm.org/cgi-bin/resolver.cgi?F3004-13R20

[15] J. Virieux, S. Operto, An overview of full-waveform inversion in exploration geophysics, GEOPHYSICS 74 (6) (2009) WCC1–WCC26. doi:10.1190/1.3238367.
URL http://library.seg.org/doi/10.1190/1.3238367